DOI: 10.1002/chem.200601022

Structure, Stability and Guest Affinity of Tris(3-ureidobenzyl)amine Capsules in Solution

Mateo Alajarín,[a] Aurelia Pastor,*[a] Raúl-Angel Orenes,[a] Eloísa Martínez-Viviente,[b, c] Heinz Rüegger,[b] and Paul S. Pregosin*[b]

Dedicated to Dr. José Antonio Abad Baños on his retirement

Abstract: In non-competitive solvents, the tris(3-ureidobenzyl)amines **1a–c** form dimeric assemblies in which guests such as CH_3CN, CH_3NO_2, CH_2Cl_2, CH_3I, CH_2BrCl, CH_2Br_2, $CHCl_3$ and C_6H_6 can be encapsulated. Variable temperature ^1H and ^1H,^1H-ROESY NMR spectroscopy, as well as pulsed-gradient spin-echo (PGSE) diffusion measurements were used to investigate the encapsulation within **1a·1a** (**1a**: tris{3-[*N*′-(4-butylphenyl)-ureido]benzyl}amine). Kinetic parameters for the encapsulation of CH_3NO_2, CH_2Cl_2 and CH_3I, both in $CDCl_3$ and in $[D_8]$toluene have been obtained by using magnetisation transfer methods. These data are discussed together with the thermodynamic parameters. The affinity between guest and capsule seems to be dictated mainly by the electronic, size and shape complementarity between cavity and guest. A gating mechanism for guest exchange is proposed.

Keywords: diffusion · encapsulation · hydrogen bonds · molecular recognition · self-assembly

Introduction

Encapsulation complexes are reversibly formed assemblies in which a small molecular guest is completely surrounded by a large molecular host, both held together by weak intermolecular forces.[1] The host/guest affinity depends on the size, shape and chemical surfaces of the species involved. For self-assembled capsules, the lifetime of the assemblies can range from milliseconds to days.[2] This time span is long enough for a variety of transformations to take place.[3] Thus, the structure of the capsule and its selectivity towards a certain guest are thermodynamically, rather than kinetically, determined. Surprisingly, relatively little quantitative information is known with respect to the kinetics and thermodynamics of encapsulation processes.[4]

It was recently shown by some of us that tris(ureidobenzyl)amines are very useful modules in supramolecular chemistry.[5] The tris(3-ureidobenzyl)amines **1a–c** (Scheme 1) associate by hydrogen bonding between the six urea functions, forming a head-to-tail directional array of 12 hydrogen bonds.[5b] The structure and existence of the self-assembled capsule **1a·1a**·CH_2Cl_2 in the solid state was confirmed by means of X-ray analysis, while NMR spectroscopy and electrospray ionisation mass spectrometry (ESIMS) data supported the persistence of the dimeric aggregates **1·1** in non-competitive solvents.[5b] Preliminary investigations of a solution of **1a·1a** in $C_2D_2Cl_4$ suggested the formation of the capsules **1a·1a**·CH_2Cl_2 and **1a·1a**·$CHCl_3$ upon addition of small amounts of CH_2Cl_2 and $CHCl_3$, respectively, to the solution.[5b]

[a] Prof. M. Alajarín, Dr. A. Pastor, R.-A. Orenes
Departamento de Química Orgánica
Facultad de Química, Universidad de Murcia
Campus de Espinardo, Murcia-30100 (Spain)
Fax: (+34) 968-364-149
E-mail: aureliap@um.es

[b] Dr. E. Martínez-Viviente, Dr. H. Rüegger, Prof. P. S. Pregosin
Laboratory of Inorganic Chemistry
ETHZ, Hönggerberg, 8093 Zürich (Schweiz)
Fax: (+41) 1-632-1090
E-mail: pregosin@inorg.chem.ethz.ch

[c] Dr. E. Martínez-Viviente
Departamento de Química Inorgánica
Facultad de Química, Universidad de Murcia
Campus de Espinardo, Murcia-30100 (Spain)

Supporting information for this article is available on the WWW under http://www.chemistry.org or from the author. It contains ^1H NMR spectra at 300 and 213 K of solutions of triurea **1a** in $CDCl_3$, with and without addition of CH_2Cl_2; more detailed descriptions of the determination of equilibrium constants, rate constants, thermodynamic parameters and activation parameters; all data for the Van't Hoff, Arrhenius and Eyring plots; VT ^1H NMR spectra of **1a·1a** in $[D_8]$toluene; ROESY spectrum at 300 K of a solution of **1a** in $[D_6]$DMSO; Figure 8 in colour.

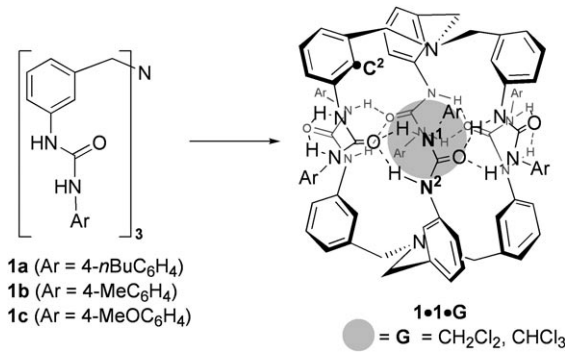

Scheme 1. Tris(3-ureidobenzyl)amines **1a–c** (left) dimerise in non-competitive solvents to form molecular capsules in which guests can be accommodated (right).

Table 1. Changes in the ^{1}H chemical shifts [ppm] of guest (**G**) and host **1a·1a** (**H**; selected resonances) upon formation of the encapsulation complex **1a·1a·G** at 213 K in $CDCl_3$ and the van der Waals volumes (V in Å^3) of each guest.

Guest	$\Delta\delta(\mathbf{G})$[a,b]	$\Delta\delta(\mathbf{H})_{N^1-H}$[a,c,d]	$\Delta\delta(\mathbf{H})_{C^2-H}$[a,c,e]	V (**G**)[f]
CH_3CN	−0.39	+0.44	+0.09	47
CH_3NO_2	−0.40	+0.52	−0.05	49
CH_2Cl_2	−0.42	+0.31	+0.06	58
CH_3I	−0.33	+0.56	+0.16	59
CH_2BrCl	−0.48	+0.26	+0.05	66
CH_2Br_2	−0.52	+0.18	+0.06	73
$CHCl_3$	−0.00	+0.00	+0.00	74

[a] From ^{1}H NMR (400 MHz) spectra. [b] $\delta\mathbf{G}_{encap}-\delta\mathbf{G}_{free}$. [c] $\delta H_{\mathbf{G}}-\delta H_{CDCl_3}$. [d] Resonances at $\delta \geq 8$ ppm, assigned to the N^1–H protons (see Scheme 1). [e] Resonances at $5.8 \geq \delta \geq 5.6$ ppm, assigned to the C^2–H protons (see Scheme 1). [f] Van der Waals volumes [Å^3]. Calculated with Hyperchem 6.01.

One of the challenges in supramolecular chemistry and, in particular, in the study of self-assembling capsules,[1] is their adequate characterization in solution.[6] Recently, pulsed-gradient spin-echo (PGSE) NMR diffusion measurements[7] proved to be useful for demonstrating encapsulation and studying the structure of hydrogen-bonded capsules in solution.[8] The diffusion coefficient, D, depends on the molecular shape and size (the larger the molecule, the lower the D value). In solution, an encapsulated guest forms a kinetic unit with the capsule. Consequently, both molecules move together and their D values will be coincident even if they have very different sizes. Encapsulation can thus be very efficiently detected by using PGSE experiments.

In this paper we show that a wide range of neutral molecules, such as CH_2ClBr, CH_3CN, CH_2Br_2, C_6H_6, CH_2Cl_2, CH_3I and CH_3NO_2, can be accommodated inside the internal cavity of **1a·1a**. PGSE[7] and magnetisation transfer methods[9] were used to investigate the encapsulation of CH_3I, CH_2Cl_2 and CH_3NO_2 in two solvents of quite different physical and chemical properties: $CDCl_3$ and [D_8]toluene. Our kinetic and thermodynamic data contribute to the understanding of the encapsulation of guests inside self-assembling hosts.

Results and Discussion

^{1}H NMR spectra: 1D ^{1}H NMR spectra of **1a·1a** in $CDCl_3$ (4–8 mM) with the addition of a 20- to 50-fold excess of guest **G** (0.14–0.27 M) were measured. The added guest partially displaces $CDCl_3$ from inside **1a·1a**,[5b] establishing an equilibrium between the assemblies **1a·1a**·$CDCl_3$ and **1a·1a·G**. Indeed, the ^{1}H NMR spectra of these solutions at room temperature show a broadening of the host signals upon addition of the guest (see Supporting Information for an example). At 213 K (Table 1 and Figure 1) the resonances of the host reveal two sets of signals that can be assigned to **1a·1a**·$CDCl_3$[10] and **1a·1a·G**. New singlets, which can be assigned to the encapsulated guest, appear at $\delta = 0.33$–0.52 ppm, shifted to lower frequency with respect to the resonances of the "free" guests. These new peaks integrate in a

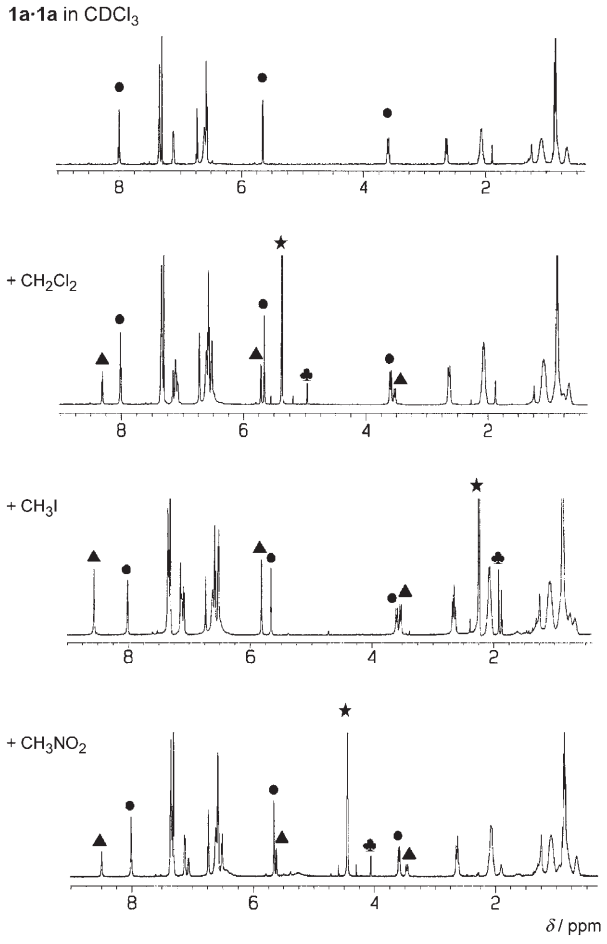

Figure 1. Sections of the ^{1}H NMR spectra at 213 K for solutions of **1a·1a** in $CDCl_3$ (2×10^{-3} M) before and after addition of a 20-fold excess of guest (CH_2Cl_2, CH_3I and CH_3NO_2). Selected peaks from **1a·1a**·$CDCl_3$ (N^1–H, C^2–H and one amine methylenic proton, see Scheme 1, and Figure S1 in the Supporting Information) are marked with circles,[10] the corresponding resonances from **1a·1a·G** are indicated with triangles, the guest within **1a·1a** is distinguished by a trefoil and the free guest with a star. The resonances from chloroform are overlapped with those of the capsule. The spectra are truncated in the upper part.

1:1 ratio with respect to the set of signals attributed to **1a·1a·G**.

For the new species **1a·1a·G** the resonance from the N^1–H urea protons, originally at approximately 8 ppm,[11] shifts to higher frequencies (see Figure 1 and Table 1). This shift suggests that the net of hydrogen bonds within **1a·1a** is strengthened by the displacement of $CDCl_3$ by any of the investigated guests, all of which have smaller van der Waals volumes than $CDCl_3$ (Table 1). Notably, the NMR chemical-shift data suggest a subtle influence of the encapsulated guest upon the structure of the capsule or, in other words, the inside of the host "feels" the presence of the guest. Thus, the resonances of the C^2–H protons, which are directed towards the cavity, slightly change with the nature of the guest (Figure 1 and Table 1).

Contrary to the results shown above, the addition of small amounts of benzene ($V=84$ Å^3),[12] toluene ($V=101$ Å^3)[12] and $C_2H_2Cl_4$ ($V=106$ Å^3)[12] to solutions of **1a·1a** in $CDCl_3$ produces no significant changes in the ^{1}H NMR spectrum of the host, either at room temperature or at low temperature. It seems that the smaller $CDCl_3$ fits better inside **1a·1a** than these added, larger molecules, and, consequently, the deuterated solvent is not displaced. In two further experiments, an excess of toluene was added to a solution of **1a·1a** in $C_2D_2Cl_4$, and an excess of $C_2H_2Cl_4$ was added to a solution of **1a·1a** in [D_8]toluene. The ^{1}H resonances from **1a·1a** in both solutions showed no changes upon addition of the second species, either at room temperature or at low temperature.[13] No new signals for either toluene or $C_2H_2Cl_4$ could be observed. To eliminate the possibility of both solvents having similar (and low) affinities for **1a·1a**, in a separate experiment **1a·1a** was dissolved in a mixture of $C_2D_2Cl_4$ and [D_8]toluene. ^{1}H NMR spectra were then recorded at 300 and 213 K. Instead of two sets of signals (for the hypothetical **1a·1a**·$C_2D_2Cl_4$ and **1a·1a**·[D_8]toluene), only one set was observed, which was assigned to the empty capsule.[14] It seems that guests with volumes exceeding 101 Å^3 cannot be associated with the host.

As the resonances for **1a·1a** in [D_8]toluene are sharper than those in $C_2D_2Cl_4$, subsequent experiments were conducted in the former solvent. The resonances from the urea protons of **1a·1a** in [D_8]toluene are shifted to higher frequencies ($\delta=8.78$, 7.84 ppm at 308 K) with respect to $CDCl_3$ ($\delta=8.12$, 6.70 ppm at 303 K). The new values might indicate a more strongly hydrogen-bonded ring of urea groups in [D_8]toluene than in $CDCl_3$. Although the lower polarity of [D_8]toluene could be playing a role in this result, we suggest that the absence of a guest inside the capsule is at least partially responsible for the stronger hydrogen bonds of the urea groups in toluene. Curiously, in this solvent the resonances from the NH protons split in two at 250 K with $\Delta\delta <$ 0.06 ppm at 400 MHz (see Figure 2 and the Supporting Information for the complete spectra). At even lower temperatures, the intensity of one of the two sets of signals increases at the expense of the other, until one of the sets almost disappears at 213 K. The possibility that the two sets of resonances would belong to empty and filled capsule was discarded, as the resonance from the C^2–H protons, at approximately 6.1 ppm, does not split (Figure 2). These protons are directed towards the cavity (Scheme 1) and would be affected by the presence of a guest. We suggest that two slightly different conformations of the empty capsule **1a·1a** exist in solution. At room temperature these two conformations would be in fast exchange. Decreasing the temperature would allow the two forms to be distinguished by means of NMR spectroscopy, while simultaneously favouring the most stable.

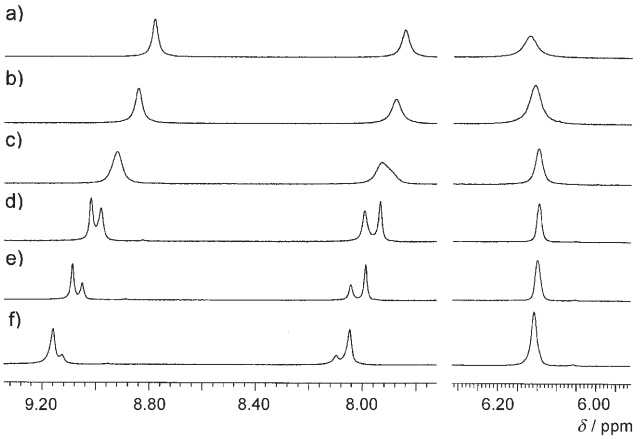

Figure 2. Two different sections of the VT ^{1}H NMR spectra (400 MHz) of **1a·1a** in [D_8]toluene (5×10^{-3} M) showing the resonances for the N^1–H protons (9.20–8.80 ppm), the N^2–H protons (8.20–7.80 ppm) and the C^2–H protons (6.10 ppm): a) 308, b) 288, c) 270, d) 250, e) 233 and f) 213 K.

We have performed encapsulation experiments with several guests in solutions of **1a·1a** in [D_8]toluene.[15] Upon addition of the guest, the ^{1}H NMR spectra at 213 K (Figure 3) show the presence of a new set of signals, assigned to **1a·1a·G**, while the resonances from the empty host, **1a·1a**, strongly decrease or even disappear. Averaged spectra are observed at 298 K (not shown). In [D_8]toluene the encapsulated guests resonate at similar frequencies to those in $CDCl_3$ (compare Figures 1 and 3).[16] This similarity of chemical shifts, in spite of the different properties of the two solvents, can be explained by the shielding effect of the host. Indeed, the free guests in [D_8]toluene resonate at approximately 1 ppm or more below their chemical shifts in $CDCl_3$.[17]

Table 2 shows an almost general decrease of the chemical shift of the N–H protons of **1a·1a** upon encapsulation of the guest in [D_8]toluene; an indication of the weakening of the hydrogen bonds within the capsule. In the series **G**= CH_2Cl_2, CH_2BrCl, CH_2Br_2 and $CHCl_3$, the larger the size of the guest, the greater the weakening of the hydrogen bonds. The C^2–H protons, directed towards the cavity, are significantly affected by the presence of the guest.

ROESY spectrum: An ^{1}H,^{1}H ROESY spectrum of **1a·1a** in $CDCl_3$ (1.1×10^{-2} M) in the presence of a 30-fold excess of CH_2Cl_2 was measured at 223 K. Under these conditions a mixture of the capsules **1a·1a**·$CDCl_3$ and **1a·1a**·CH_2Cl_2

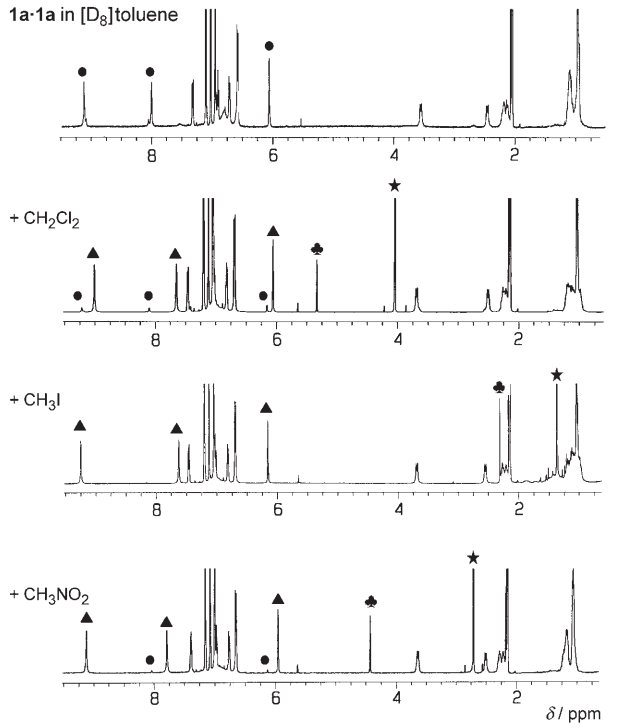

Figure 3. Sections of the ^{1}H NMR spectra at 213 K for solutions of **1a·1a** in [D_8]toluene (2×10^{-3} M), before and after addition of a 20-fold excess of guest (CH_2Cl_2, CH_3I and CH_3NO_2). Selected peaks from **1a·1a** (N^1–H, N^2–H and C^2–H, see Scheme 1, and Figure S1 in the Supporting Information) are marked with circles, the corresponding resonances from **1a·1a·G** are indicated with triangles, the encapsulated guest is distinguished by a trefoil and the free guest with a star. The spectra are truncated in the upper part.

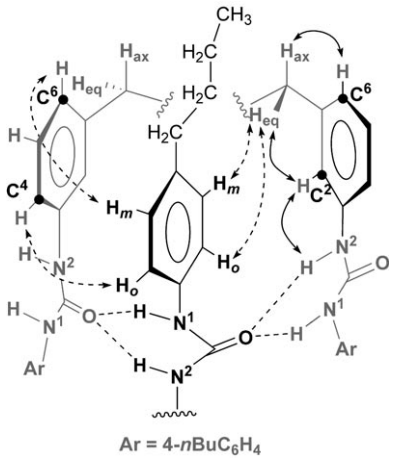

Figure 4. Intramolecular (solid arrows) and intermolecular (dashed arrows) ROE interactions found within the dimeric capsules **1a·1a** in the ^{1}H,^{1}H ROESY spectrum of a solution in $CDCl_3$ (1.1×10^{-2} M), in the presence of a 30-fold excess of CH_2Cl_2, at 223 K.

Table 2. Changes in the ^{1}H chemical shifts [ppm] of guest (**G**) and host **1a·1a** (H; selected resonances) upon formation of the encapsulation complex **1a·1a·G** at 213 K in [D_8]toluene and the van der Waals volumes (V in Å^3) of each guest.

Guest	$\Delta\delta(\mathbf{G})$[a,b]	$\Delta\delta(H)_{N^1-H}$[a,c,d]	$\Delta\delta(H)_{N^2-H}$[a,c,e]	$\Delta\delta(H)_{C^2-H}$[a,c,f]	V (**G**)[g]
CH_3CN	+1.48	−0.09	−0.32	−0.06	47
CH_3NO_2[h]	+1.71	−0.02	−0.26	−0.18	49
CH_2Cl_2	+1.30	−0.21	−0.45	−0.10	58
CH_3I[h]	+0.95	+0.05	−0.46	−0.01	59
CH_2BrCl	+1.21	−0.27	−0.60	−0.11	66
CH_2Br_2	+1.16	−0.34	−0.70	−0.10	73
$CHCl_3$	–[i]	−0.48	–[j]	−0.18	74
C_6H_6	–[i]	−0.23	–[j]	−0.19	84

[a] From ^{1}H NMR (400 MHz) spectra. [b] $\delta\mathbf{G}_{encap}-\delta\mathbf{G}_{free}$. [c] $\delta H_{\mathbf{G}}-\delta H_{empty}$. [d] Resonances at $\delta\geq8.7$ ppm, assigned to the N^1–H protons (see Scheme 1). [e] Resonances at $8.2>\delta>7.3$ ppm, assigned to the N^2–H protons (Scheme 1). [f] Resonances at $6.2>\delta>5.8$ ppm, assigned to the C^2–H protons (see Scheme 1). [g] Calculated with Hyperchem 6.01. [h] At this concentration only the resonances of the filled capsule were observed. [i] The resonance from the encapsulated guest overlaps with those due to the aromatic protons of **1a·1a** and **1a·1a·G**. [j] The resonances from the N^2–H protons in **1a·1a·G** overlap with those due to the aromatic protons of **1a·1a** and **1a·1a·G**.

exists, with the latter being the major species. Figure 4 shows the most significant intramolecular and intermolecular ROE contacts found within the dimeric capsules **1a·1a·G**. Figure 5 shows the relevant sections of the ROESY spectrum.

Intramolecular ROE contacts are found within each molecule of **1a** between the aromatic C^6–H protons at approximately 7.1 ppm and only one of the two non-equivalent methylenic protons of the amine moiety (at approximately 2.6 ppm, Figure 5a). Consequently, these methylenic protons are assigned as being in a "pseudoaxial" position ($C-H_{ax}$ bond parallel to the C_3 axis of the dimer). The "pseudoequatorial" methylenic protons at 3.5–3.6 ppm (H_{eq}) show intramolecular ROE cross peaks with the aromatic C^2–H protons at approximately 5.6–5.7 ppm (also in Figure 5a). Figure 5b shows ROE cross peaks between the same C^2–H protons and the resonances at 6.74 ppm (for **1a·1a·**$CDCl_3$) and 7.18 ppm (for **1a·1a·**CH_2Cl_2), which supports the previous assignment of these peaks to the N^2–H protons. Additionally, the ROESY spectrum also shows cross peaks between the two molecules of **1a** in each capsule (Figure 5a, c). These intermolecular contacts confirm the capsular structure of **1a·1a**, because the aromatic protons of the *p*-butylphenyl groups of one molecule of **1a** interact via ROE with the tribenzylamine moiety of the second molecule.[18] Undoubtedly, the most relevant signal in the ROESY spectrum is shown in Figure 6: a cross peak between the resonance assigned to the encapsulated CH_2Cl_2 (at 4.95 ppm) and the C^2–H protons of **1a·1a·**CH_2Cl_2 (at ca. 5.70 ppm). This is consistent with the presence of a guest molecule of CH_2Cl_2 inside the cavity of **1a·1a**. No other cross peaks between the encapsulated guest and the host were found.

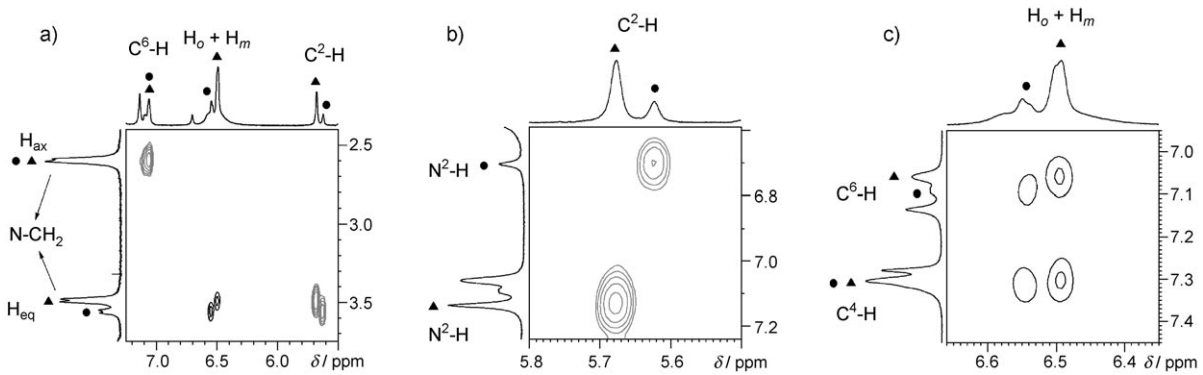

Figure 5. Three different sections of the ^{1}H,^{1}H ROESY spectrum of a solution of **1a·1a** in $CDCl_3$ (1.1×10^{-2} M) in the presence of a 30-fold excess of CH_2Cl_2, measured at 223 K. Selected peaks from **1a·1a**·$CDCl_3$ are marked with circles, and the corresponding peaks from **1a·1a**·CH_2Cl_2 are marked with triangles. The ROE cross peaks due to intramolecular interactions (within one molecule of **1a**) are in grey, while those due to intermolecular interactions between the two molecules of **1a** in each capsule are in black. The three sections have the same plotting cut-off levels.

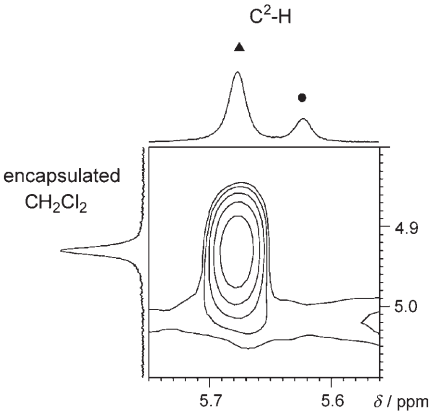

Figure 6. Section of the ^{1}H,^{1}H ROESY spectrum of a solution of **1a·1a** in $CDCl_3$ (1.1×10^{-2} M) in the presence of a 30-fold excess of CH_2Cl_2, at 223 K. The cross peak relating the resonances assigned to the encapsulated CH_2Cl_2 and the C^2–H protons of **1a·1a**·CH_2Cl_2 (marked with a triangle) is shown. The resonance of the C^2–H protons of **1a·1a**·$CDCl_3$ is marked with a circle. The plotting cut-off levels are the same as those in Figure 5.

^{1}H PGSE diffusion investigations: We carried out ^{1}H PGSE diffusion measurements on solutions of **1a·1a** in $CDCl_3$ plus a 20-fold excess of **G**, where **G** = CH_3NO_2, CH_2Cl_2 and CH_3I, at 300 and 213 K. At the lower temperature, the intensity decays were followed on the separate resonances marked in Figure 1. The average peaks were used at 300 K. The results are shown in Table 3, in which the hydrodynamic radii have been calculated from the D values by using the Stokes–Einstein equation.[19]

At 300 K, the D values measured for the average signal of the capsule (from **1a·1a**·$CDCl_3$ and **1a·1a·G**) are similar for the three guests ($D = 4.63 \pm 0.02$). The result is the same for **1a·1a**·$CDCl_3$ in the absence of added guest. The coincidence is not surprising, as the presence of a guest is not expected to affect the size of the resulting host complex. The calculated r_H value is 9.0 ± 0.1 Å, which is in good agreement with the size estimated from the X-ray structure determination.[20]

Table 3. Diffusion coefficients, D ($\times10^{-10}$ m^{2}s^{-1}), and hydrodynamic radii, r_H [Å], for solutions of **1a·1a** (2×10^{-3} M) plus a 20-fold excess of guest (**G**) in $CDCl_3$.[a]

	300 K			
	1a·1a (average)[b]		**G** (average)[c]	
Guest	D[d]	r_H[e]	D[d]	r_H[e,f]
($CDCl_3$)	4.63	9.0	–	–
CH_2Cl_2	4.63	9.0	26.6	1.6 (2.8)
CH_3NO_2	4.61	9.0	25.7	1.6 (2.9)
CH_3I	4.65	8.9	25.4	1.6 (2.9)

	213 K							
	1a·1a·$CDCl_3$[g]		**1a·1a·G**[g]		Encap **G**		Free **G**	
Guest	D[d]	r_H[e]	D[d]	r_H[e]	D[d]	r_H[e]	D[d]	r_H[e]
($CDCl_3$)	0.885	9.4	–	–	–	–	–	–
CH_2Cl_2	0.894	9.3	0.889	9.4	0.880	9.5	6.08	1.4
CH_3NO_2	0.884	9.4	0.881	9.5	0.881	9.5	5.17	1.6
CH_3I	0.895	9.3	0.892	9.3	0.894	9.3	5.43	1.5

[a] $\eta(CHCl_3,\ 300\ K) = 0.529\times10^{-3}$ Kg s^{-1} m^{-1}; $\eta(CHCl_3,\ 213\ K) = 1.87\times10^{-3}$ Kg s^{-1} m^{-1}. The peak from the chloroform solvent is masked by the resonances from **1a·1a**. [b] The resonances from **1a·1a**·$CDCl_3$ and **1a·1a·G** are not resolved at 300 K when **G** = CH_2Cl_2 and CH_3NO_2 (the D value measured on the average resonances of **1a·1a** is given). For **G** = CH_3I, the average of the D values measured on the separate resonances of **1a·1a**·CH_3I ($D = 4.64\times10^{-3}$ m^{2}s^{-1}) and **1a·1a**·$CDCl_3$ ($D = 4.66\times10^{-3}$ m^{2}s^{-1}) is given. [c] The resonances from the encapsulated and free guest are not resolved. [d] Experimental error is less than ±2%. [e] Standard deviation is approximately ±0.1 Å. [f] The radii calculated by using a factor 3.4 instead of 6 in the Stokes–Einstein equation are given in parentheses (see ref. [19]). [g] The average of the D values measured for the three resonances marked in Figure 1, is given. These D values were identical within the experimental error.

The observed average resonance for the guests at 300 K stems mainly from the free guest molecules (the contribution of **1a·1a·G**, is very small, as **G** is added in a 20-fold excess with respect to **1a·1a**). Consequently, the measured average D values for the guests at 300 K are, as expected, much larger than those for **1a·1a**, and the r_H values are, correspondingly, much smaller.[19] No significant difference in size between the three guests can be detected by using this method. At 213 K, the D values for the host **1a·1a** in the presence of CH_3NO_2, CH_2Cl_2 or CH_3I are all identical

within the experimental error ($D = 0.889 \pm 0.01 \times 10^{-10}\,m^2s^{-1}$). This diffusion coefficient is much smaller than the value found at 300 K, owing to the higher viscosity of the solvent at the lower temperature. The calculated hydrodynamic radius compensates for the change in viscosity,[19] and affords a value of 9.4 ± 0.1 Å, which is in fairly good agreement with the estimation at 300 K.[21] But the most interesting diffusion data in Table 3 correspond to the measurements on the resonances assigned to the encapsulated guests at 213 K. The D values for these signals (0.880, 0.881 and $0.894 \times 10^{-10}\,m^2s^{-1}$) are all identical, within experimental error, and close to those of **1a·1a**, clearly confirming that the host and guest exist together in solution as a single unit. For the resonances of the free guests the D values are much larger.

Figure 7 shows a plot of the diffusion results at 213 K for a solution of **1a·1a** in $CDCl_3$ plus a 20-fold excess of CH_3I. The coincidence of the D value for the capsules **1a·1a**·$CDCl_3$ and **1a·1a**·CH_3I and the encapsulated CH_3I can be clearly appreciated, while the free CH_3I moves much faster.

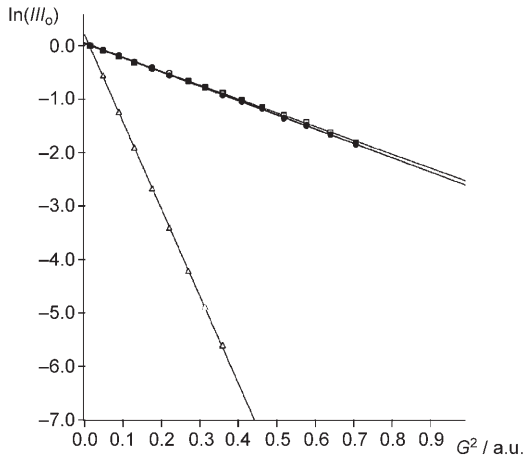

Figure 7. Plot of $\ln(I/I_o)$ versus arbitrary units proportional to the square of the gradient amplitude, for a ^1H PGSE diffusion measurement of a 2×10^{-3} M solution of **1a·1a** in $CDCl_3$ plus a 20-fold excess of CH_3I. The measurements on the resonances of the capsule in **1a·1a**·$CDCl_3$ (○) and **1a·1a**·CH_3I (●), as well as on the resonance from the encapsulated CH_3I (□) afford very similar intensity decays, while on the resonance from the free CH_3I (△) the intensity decay is much stronger, indicating a much larger D value. Diffusion parameters (see the Experimental Section): $\Delta = 65.5$ ms, $\delta = 4.5$ ms, number of scans = 40.

^1H PGSE diffusion measurements have also been performed on solutions of **1a·1a** in $[D_8]$toluene plus the same guests (**G** = CH_3I, CH_2Cl_2, and CH_3NO_2). The results are shown in Table 4. As expected, the free guest and the solvent move much faster than the host. As in Table 3, the presence of the guests does not significantly affect the D values for the host in $[D_8]$toluene ($4.39 \pm 0.05 \times 10^{-10}\,m^2s^{-1}$ at 300 K and $0.537 \pm 0.004 \times 10^{-10}\,m^2s^{-1}$ at 213 K). Yet again, the most important information comes from the measurements on the resonances from the encapsulated guest, at 213 K, which afford the same D values as the host. This result clearly shows again that each host–guest assembly acts as a kinetic unit in solution. The calculated hydrodynamic radii are slightly larger in $[D_8]$toluene than in $CDCl_3$.

Table 4. Diffusion coefficients, D ($\times 10^{-10}\,m^2s^{-1}$), and hydrodynamic radii, r_H [Å], for solutions (2×10^{-3} M) of **1a·1a** plus a 20-fold excess of guest (**G**) in $[D_8]$toluene.

	300 K					
	1a·1a (average)[a]		**G** (average)[b]		Toluene	
Guest	D[c]	r_H[d]	D[c]	r_H[d,e]	D[c]	r_H[d,f]
–	4.34	9.4	–	–	20.5	2.0 (3.4)
CH_2Cl_2	4.38	9.3	27.2	1.5 (2.8)	20.8	1.9 (3.4)
CH_3NO_2	4.37	9.3	26.7	1.5 (2.9)	20.8	2.0 (3.4)
CH_3I	4.43	9.2	26.7	1.5 (2.8)	20.7	2.0 (3.4)

	213 K									
	1a·1a		**1a·1a·G**		Encap **G**		Free **G**		Toluene	
Guest	D[c]	r_H[d]	D[c]	r_H[d]	D[c]	r_H[d]	D[c]	r_H[d]	D[c]	r_H[d]
–	0.533	9.8	–	–	–	–	–	–	2.88	1.8
CH_2Cl_2	0.538	9.8	0.538	9.8	0.541	9.7	4.39	1.2	2.93	1.8
CH_3NO_2	–[g]	–	0.533	9.8	0.535	9.8	4.14	1.3	2.92	1.8
CH_3I	–[h]	–	0.533	9.8	0.539	9.7	3.94	1.3	2.91	1.8

[a] η(toluene, 300 K) = 0.537×10^{-3} Kg s^{-1} m^{-1}; η(toluene, 213 K) = 2.97×10^{-3} Kg s^{-1} m^{-1}. The resonances from the empty capsule **1a·1a** and the capsule with guest (**1a·1a·G**) are not resolved at 300 K. The D value measured on the average signal of **1a·1a** is given. [b] The resonances from the encapsulated and free guest are not resolved. [c] Experimental error is approximately ±2%. [d] Standard deviation is approximately ±0.1 Å. [e] The radii calculated by using a factor 3.2 instead of 6 in the Stokes–Einstein equation are shown in parentheses. [f] The radii calculated by using a factor 3.5 instead of 6 in the Stokes–Einstein equation are shown in parentheses (see ref. [19]). [g] The signals for the empty capsule **1a·1a** are too weak for measuring its D value. [h] No signals for the empty capsule **1a·1a** can be detected.

Diffusion measurements on a sample of only the solvent $[D_8]$toluene (on the residual proton resonance) afforded D values of $21.0 \times 10^{-10}\,m^2s^{-1}$ at 300 K and $2.97 \times 10^{-10}\,m^2s^{-1}$ at 213 K, similar to those given for this solvent in Table 4. Consequently, the presence of **1a·1a**, at least at our relatively low concentrations, does not affect the diffusion of the solvent. A similar comparison with $CDCl_3$ was not possible, due to overlap with resonances from **1a·1a**.

Finally, we investigated a solution of **1a** in $[D_6]$DMSO (2×10^{-3} M). In this strongly hydrogen-bonding solvent, **1a** exists as a monomeric, non-assembled species.[5b] The measured D value, $1.28 \times 10^{-10}\,m^2s^{-1}$, corresponds to r_H = 9.0 Å,[22] which is, surprisingly, the same hydrodynamic radius as found for the dimer **1a·1a** in $CDCl_3$. We have previously reported D values in $[D_6]$DMSO for related compounds,[5d] and found that solvation and/or hydrogen bonding by $[D_6]$DMSO produces an increase in the hydrodynamic radius of the solute of approximately 1 Å with respect to $CDCl_3$. With this information, a "corrected" r_H value for monomeric **1a** would be approximately 8 Å, which is in better agreement with an estimation made with the Chem3D modelling software (8.1 Å).

Molecular modelling: We have attempted a simple molecular modelling investigation on our tris(3-ureidobenzyl)-

amine-derived capsules, by using the program MacroModel 8.1 (AMBER* force field). For simplicity, the pendant *n*-butyl chains of **1a** have been replaced by methyl groups, as in **1b** (Scheme 1). We have focused on the empty dimer **1b·1b** and the capsules **1b·1b**·CH_3NO_2, **1b·1b**·CH_2Cl_2, **1b·1b**·CH_3I and **1b·1b**·$CHCl_3$, in the presence of $CDCl_3$ as the solvent (Figure 8).

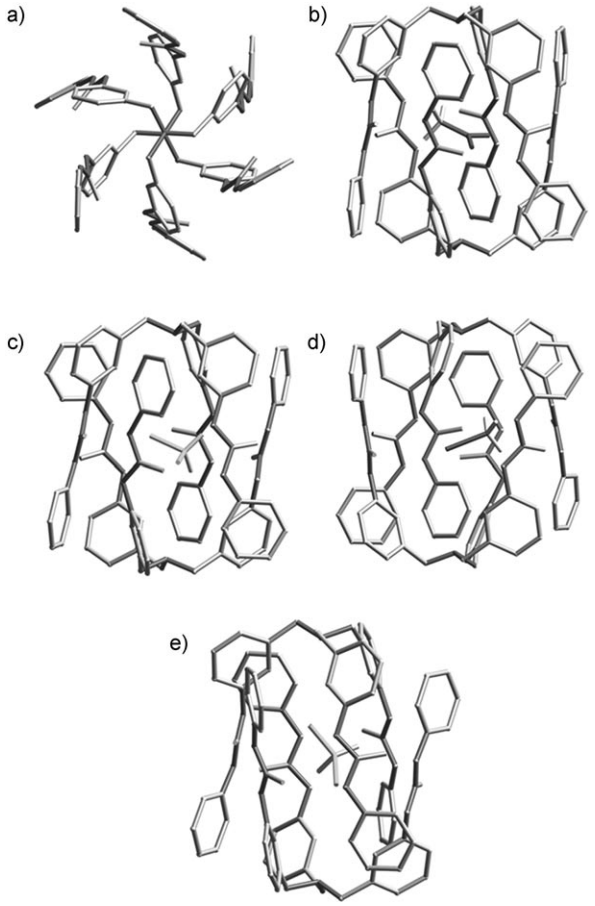

Figure 8. Energy-minimized structures (MacroModel 8.1, AMBER* force field) of a) **1b·1b**, b) **1b·1b**·CH_3NO_2, c) **1b·1b**·CH_2Cl_2, d) **1b·1b**·CH_3I and e) **1b·1b**·$CHCl_3$. All hydrogen atoms and methyl groups of the *p*-tolyl fragments have been omitted for clarity.

The lowest energy conformation for **1b·1b** was determined by Monte Carlo multiple minimisation. Each of the four guests was then placed inside this structure and a new calculation was performed to obtain the minimised structures of the filled capsules. The empty dimer **1b·1b** shows a perfect S_6 symmetry with a distance between the two pivotal, amine nitrogen atoms of 10.04 Å (Figure 8a). The hydrogen bonds involving the terminal nitrogen atom of the urea functionality (N^1 in Scheme 1) are stronger than those involving N^2: $d(N^1\cdots O{=}C) = 2.78$ and $d(N^2\cdots O{=}C) = 2.90$–2.91 Å ($d$ = distance). The S_6 symmetry is broken in **1b·1b**·CH_3NO_2 (Figure 8b) although an averaged structure is expected in solution. The presence of the guest CH_3NO_2 does not affect the separation between the two subunits; the distance between the two amine nitrogen atoms (10.07 Å) being similar to the value found in the empty dimer. As for the hydrogen bonds, they are slightly weakened by the presence of the guest, with those involving N^2 being more affected than those involving N^1: $d(N^1\cdots O{=}C) = 2.78$–2.82 Å and $d(N^2\cdots O{=}C) = 2.83$–3.16 Å.

The encapsulation of the larger guests CH_2Cl_2, CH_3I and $CHCl_3$ (Figure 8c–e) leads to an increase in the distance between the two amine nitrogen atoms ($d(N\cdots N) = 10.14$ Å, 10.26 Å and 10.76 Å, respectively) with respect to **1b·1b** and **1b·1b**·CH_3NO_2. Similarly, the hydrogen bonds in **1b·1b**·CH_2Cl_2, **1b·1b**·CH_3I, and **1b·1b**·$CHCl_3$ are significantly weakened and, again, those involving N^2 are more strongly affected (for CH_2Cl_2: $d(N^1\cdots O{=}C) = 2.78$–2.83 Å and $d(N^2\cdots O{=}C) = 2.92$–3.45 Å; for CH_3I: $d(N^1\cdots O{=}C) = 2.76$–2.82 Å and $d(N^2\cdots O{=}C) = 2.85$–3.62 Å; for $CHCl_3$: $d(N^1\cdots O{=}C) = 2.74$–2.85 Å and $d(N^2\cdots O{=}C) = 2.93$–3.80 Å).[23]

In conclusion, the hydrogen bonds involving N^1 are the strongest and least affected by encapsulation. These observations support the assignment of the proton resonance at higher frequency to the N^1–H protons, which was based on the ROESY spectrum of **1a·1a**·CH_2Cl_2 (see above). In toluene (Table 2) this N^1–H resonance is less sensitive to the presence of an encapsulated guest ($|\Delta\delta| = 0.02$–0.48 ppm) than the N^2–H resonance ($|\Delta\delta| = 0.26$–0.70 ppm).

Equilibria: To gain insight into the mechanism of the encapsulation process, we have investigated the kinetics and thermodynamics of the equilibria according to Equations (1) and (2) (in $CDCl_3$ and [D_8]toluene, respectively):

$$\mathbf{1a}\cdot\mathbf{1a}\cdot CDCl_3 + \mathbf{G} \underset{k_I}{\overset{k_D}{\rightleftharpoons}} \mathbf{1a}\cdot\mathbf{1a}\cdot\mathbf{G} + CDCl_3 \quad (1)$$

$$\mathbf{1a}\cdot\mathbf{1a} + \mathbf{G} \underset{k_I}{\overset{k_D}{\rightleftharpoons}} \mathbf{1a}\cdot\mathbf{1a}\cdot\mathbf{G} \quad (2)$$

in which $\mathbf{G} = CH_2Cl_2$, CH_3I, CH_3NO_2, and k_D and k_I are the rate constants for the forward and the reverse reactions, respectively. CH_2Cl_2, CH_3I and CH_3NO_2 were chosen as guests, because they form the most stable complexes.

Thermodynamic data: At temperatures between approximately 228 and 273 K the equilibria shown in Equations (1) and (2) are slow on the NMR time scale, affording separate resonances for the involved species. The association constants in this range of temperatures have been determined from the integrals of the separate peaks (see the Supporting Information). From a Van't Hoff plot ($\ln K_a$ vs. $1/T$) we have calculated the thermodynamic parameters ΔH and ΔS, assuming that they are not temperature dependent. The results are shown in Table 5, together with the ΔG values at 298, 273 and 213 K.

The values found for ΔG reflect some of the facts previously observed in the ^{1}H NMR spectra shown in Figures 1 and 3: Thus, 1) ΔG for Equations (1) and (2) is always negative and, indeed, the encapsulation of the guest takes place, as shown by the ^{1}H NMR spectra and 2) the largest $|\Delta G^{213}|$, in both solvents, is found for CH_3I, for which the degree of encapsulation is seen to be larger (i.e., for the same concen-

Table 5. Thermodynamic parameters for the reactions shown in Equation (1) ($CDCl_3$) and Equation (2) ([D_8]toluene).

Solvent	Guest	ΔH[a]	ΔS[b]	ΔG_{298}[a]	ΔG_{273}[a]	ΔG_{213}[a]
$CDCl_3$	CH_3NO_2	0.0	42.6	−12.7	−11.6	−9.1
$CDCl_3$	CH_2Cl_2	−2.6	28.8	−11.2	−10.5	−8.7
$CDCl_3$	CH_3I	−6.8	22.0	−13.3	−12.8	−11.5
[D_8]toluene	CH_3NO_2	−8.8	14.9	−13.2	−12.8	−11.9
[D_8]toluene	CH_2Cl_2	−14.8	−19.3	−9.1	−9.5	−10.7
[D_8]toluene	CH_3I	−21.4	−29.0	−12.8	−13.5	−15.2

[a] In kJ mol^{-1}. [b] In J K^{-1} mol^{-1}.

tration of added guest the ratio **1a·1a·G/1a·1a**·$CDCl_3$ or **1a·1a·G/1a·1a** is larger for CH_3I). The encapsulation of the three guests is enthalpically favoured, both starting from an empty capsule [in [D_8]toluene, Eq. (2)] or when a $CDCl_3$–guest exchange takes place [Eq. (1)]. The only exception is the exchange of $CDCl_3$ by CH_3NO_2, which is energetically neutral ($\Delta H = 0.0$ kJ mol^{-1}). Generally speaking, a "filled" capsule is favoured over an empty host because of the attractive capsule–guest interactions (in our case, mainly van der Waals forces).[4a,24] The larger $|\Delta H|$ values for Equation (2) than for Equation (1) are in agreement with this principle. These attractive interactions between guest and host may compensate for the weakening of the hydrogen bonds within **1a·1a** upon encapsulation of the guest. In $CDCl_3$, the clearly favourable ΔH values for the exchange of $CDCl_3$ by CH_2Cl_2 and CH_3I suggest a stronger affinity of the capsule for these two guests than for $CDCl_3$.

The data in Table 5 also indicate that the encapsulation of the guest is enthalpically favoured in the order $CH_3I > CH_2Cl_2 > CH_3NO_2$, both in $CDCl_3$ and [D_8]toluene, in spite of the different polar and hydrogen-bonding characteristics of the two solvents. Thus, the guest–solvent interaction does not seem to be playing an important role in the relative ΔH values. The ability of the guest to hydrogen bond with the capsule does not seem to be a determining factor either, as CH_3NO_2 should then probably be the most favoured. Consequently, the affinity between guest and capsule seems to be dictated mainly by the electronic, size and shape characteristics of guest and cavity.

It is known that the optimum packing coefficient in encapsulation complexes is 55 %.[25] Thus, the van der Waals volume of CH_3I (59 Å^3, Table 1, entry 4) may be used to roughly estimate the volume of the cavity in **1a·1a**. The result, approximately 110 Å^3, is intermediate between the values for the tennis ball (50–55 Å^3)[4a] and the tetraureidocalix[4]arene dimers (210 Å^3)[26] reported by Rebek.

Some of the entropy data in Table 5 also support the initial situation of an empty capsule in [D_8]toluene [Eq. (2)]. Thus, in this solvent, ΔS is strongly negative for the encapsulation of CH_2Cl_2 and CH_3I, while for the same guests in $CDCl_3$ ΔS is positive, suggesting that the liberation of $CDCl_3$ completely compensates for the loss of entropy produced by the encapsulation of the added guest. Only the positive value of ΔS for the encapsulation of CH_3NO_2 in [D_8]toluene is difficult to understand, and might be related to more subtle thermodynamic contributions, such as specific heat and/or volume differences between the capsule and their separated components, that is, dimer and guest. The trend in ΔS is $CH_3NO_2 > CH_2Cl_2 > CH_3I$ in the two solvents investigated. The formation of **1a·1a**·CH_3NO_2 might be entropically favoured due to its somewhat smaller size, which would allow a greater mobility of the guest within the capsule than for the larger CH_3I and CH_2Cl_2. These two guests, additionally, could distort the structure of the capsule more significantly than CH_3NO_2.

The decreasing order in ΔS is the opposite to that for $|\Delta H|$, showing a compensation between the entropic and enthalpic factors. A plot of ΔH versus ΔS (Figure 9) gives a

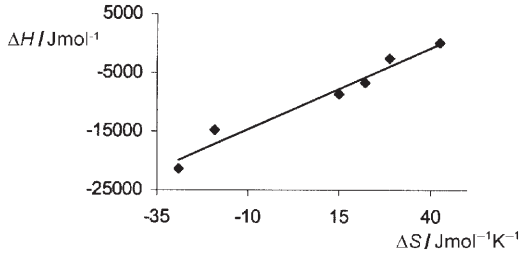

Figure 9. Plot of ΔH versus ΔS for the encapsulation of CH_3I, CH_2Cl_2 and CH_3NO_2 inside **1a·1a** in both solvents, $CDCl_3$ and [D_8]toluene.

good linear correlation ($R = 0.96$) with a slope of 276 K (T_c).[27,28] As ΔH becomes more negative (stronger interactions), ΔS tends to decrease due to the lower freedom in the system, and vice versa.[29] This compensation between enthalpy and entropy has been repeatedly observed for the association between a receptor and a ligand for a great number of systems.[27b,30]

Kinetic data: Using magnetisation transfer techniques, we have measured the rate constants k_D and k_I for Equations (1) and (2) at several low temperatures (see the Supporting Information). From these data we have derived the activation parameters for the forward and reverse reactions, as given in Table 6.

Table 6. Activation parameters for the forward and reverse encapsulation reactions shown in Equation (1) (in $CDCl_3$) and Equation (2) (in [D_8]toluene).

		Forward reaction				Reverse reaction			
Solvent	Guest	E_A[a]	$\Delta H^{\neq}$[a]	$\Delta S^{\neq}$[b]	$\Delta G^{\neq}_{298}$[a]	E_A[a]	$\Delta H^{\neq}$[a]	$\Delta S^{\neq}$[b]	$\Delta G^{\neq}_{298}$[a]
$CDCl_3$	CH_3NO_2	56.6	54.5	−27.6	62.7	56.0	53.9	−26.4	61.8
$CDCl_3$	CH_2Cl_2	54.0	51.9	−43.5	64.9	56.8	54.7	−23.2	61.6
$CDCl_3$	CH_3I	70.7	68.4	2.7	67.6	78.4	76.1	32.2	66.5
[D_8]toluene	CH_3NO_2	56.1	54.0	−46.9	68.0	61.1	59.0	−14.2	63.2
[D_8]toluene	CH_2Cl_2	51.1	49.0	−63.5	67.9	61.4	59.2	−4.75	60.6
[D_8]toluene	CH_3I	61.1	58.9	−51.5	74.2	69.2	66.9	−8.67	69.5

[a] In kJ mol^{-1}. [b] In J K^{-1} mol^{-1}.

The activation energies (E_A and $\Delta H^{\neq}$) for Equations (1) and (2) increase in the order $CH_2Cl_2 < CH_3NO_2 < CH_3I$ for the forward reaction, while for the reverse process $CH_2Cl_2 \cong CH_3NO_2 \ll CH_3I$. The trend is the same in both solvents, again discarding the solvent–guest interactions as a major differentiating factor. All the activation enthalpies ($\Delta H^{\neq}$) are high and positive, probably because a partial or total rupture of the hydrogen-bonded ring of urea molecules is necessary for the inclusion/exclusion of the guests.

The activation entropies for the forward reactions in [D_8]toluene [Eq. (2)] are strongly negative, as expected for a process in which two species, host and guest, are brought together. In $CDCl_3$, the strong differences in the $\Delta S^{\neq}$ for CH_3NO_2 and CH_2Cl_2, both negatives, and CH_3I, which is positive, suggest some change in the mechanism of the process, due to the different properties of the guests.

The inclusion/exclusion of the guest from the capsule may take place by: 1) a *dissociation–recombination mechanism*, in which a complete dissociation of the capsule takes place, or 2) a *gating mechanism*, in which a temporary gate is opened by partial dissociation of the capsule, allowing the guest to come in or out. Interestingly, the exchange of **1a** by **1c** in a solution of homodimers **1a·1a**, **1c·1c** and heterodimer **1a·1c** is slow on the NMR time scale at room temperature,[31] while the inclusion/exclusion of a guest in **1a·1a** is fast. These observations point to a gating mechanism for the guest exchange,[32] as was also found for Rebek's tennis ball,[4e] softballs[33] and cylindrical capsules.[34] In contrast, the exchange of benzene in tetraureidocalix[4]arene dimers requires capsule dissociation.[4c]

Conclusions

Tris(3-ureidobenzyl)amines **1a** form self-assembling dimeric aggregates **1a·1a** in $CDCl_3$ and [D_8]toluene, in which organic molecules of adequate size and shape, such as CH_3CN, CH_3NO_2, CH_2Cl_2, CH_3I, CH_2BrCl, CH_2Br_2, $CHCl_3$ and C_6H_6, can be accommodated. Variable temperature ^{1}H and ^{1}H,^{1}H-ROESY NMR experiments have been used to investigate these **1a·1a·G** assemblies. Thus, new resonances for capsule and guest in **1a·1a·G** have been detected upon addition of the guests to solutions of **1a·1a** in $CDCl_3$ and [D_8]toluene. PGSE diffusion measurements have been used to further investigate the solutions in which **G** = CH_3NO_2, CH_2Cl_2 and CH_3I. The results show that capsule and guest in **1a·1a·G** form a kinetic unit in solution.

Thermodynamic and kinetic parameters for the encapsulation of CH_3NO_2, CH_2Cl_2 and CH_3I into **1a·1a** in $CDCl_3$ and [D_8]toluene have also been determined. Similar trends in the thermodynamic parameters were found for the encapsulation of each guest in both solvents, pointing to the affinity between guest and **1a·1a** being dictated mainly by the electronic, size and shape complementarity between guest and cavity. The thermodynamic data also support the initial situation of an empty capsule in [D_8]toluene. Interestingly, a compensation between enthalpic and entropic effects has been observed. A gating mechanism is proposed for the guest exchange.

Experimental Section

PGSE NMR diffusion measurements: The PGSE NMR diffusion measurements were carried out by using the stimulated echo pulse sequence,[7b] as it has been explained elsewhere.[35] All the experiments were performed on a 500 MHz Bruker AVANCE spectrometer, equipped with a microprocessor-controlled gradient unit and a multinuclear inverse probe with an actively shielded *Z*-gradient coil. The measurements were carried out without spinning. The shape of the gradient pulse was rectangular, and its strength was varied automatically during the course of the experiments. The *D* values were determined from the slope of the regression line $\ln(I/I_o)$ versus G^2, according to Equation (3) in which I/I_o = observed spin echo intensity/intensity without gradients, G = gradient strength, Δ = delay between the midpoints of the gradients, D = diffusion coefficient, γ = gyromagnetic ratio and δ = gradient length. The calibration of the gradients was carried out by means of a diffusion measurement of HDO in D_2O ($D_{HDO} = 1.9 \times 10^{-9}\ m^2\ s^{-1}$).[36]

$$\ln\left(\frac{I}{I_o}\right) = -(\gamma\delta)^2 G^2 \left(\Delta - \frac{\delta}{3}\right) D \qquad (3)$$

The precise temperatures were determined by introducing a thermocouple inside the bore of the magnet, before and after the measurements. For the experiments at 300 K the airflow was disconnected, to avoid perturbations of the mechanical stability of the sample. In the experiments at 233 K, the onset of convection currents due to the cooling N_2 flow was avoided by the use of two commercially available coaxial NMR tubes, separated by air, and kept concentric by a Pyrex spacer.[37] The inner tube had an internal diameter of 1.96 mm and an external diameter of 2.97 mm. A standard 5 mm vessel was used for the outer tube. The values reported in Tables 3 and 4 are the average of three different measurements, which yielded *D* values within a maximum of ±1.5% of the reported one. All the measurements were carried out by using the ^{1}H resonances. Typically, 14–20 points were used for the regression analysis and the experimental time was between approximately 30 min and 3 h. A relaxation delay of 5 s was routinely used. All of the observed data leading to the reported *D* values afforded lines whose correlation coefficients were above 0.999. Based on our experience of diffusion over several years, we propose an experimental error of ±2% for the *D* values and a standard deviation of ±0.1 Å for the hydrodynamic radii.

For the measurements in $CDCl_3$ and [D_8]toluene the gradient length, δ, was set to 1.75 ms and the diffusion delay was approximately 68, 118 or 168 ms. The number of scans was usually 16 to 28. The only exceptions were the measurements on the signals of the solvent or guests, where shorter diffusion delays, approximately 27 ms, were used, to compensate for the higher mobility of these small molecules. Eight scans were enough for these intense signals. At 213 K, due to the smaller volume of the sample, the number of scans was between 40 and 100. The δ values were higher than those at room temperature (3–5 ms), to compensate for the decreased mobility (weaker intensity decay) of the molecules at low temperature. Typically, the diffusion delays were 36, 65.5, 90, 164 or 213.5 ms. In [D_6]DMSO, the high viscosity of the solvent was also compensated by a longer gradient length (2–3.5 ms).

ROESY experiment: The ROESY spectrum was measured on a 1.1×10^{-2} M solution of **1a·1a** in $CDCl_3$ in the presence of a 30-fold excess of CH_2Cl_2, by using a 600 MHz Bruker AVANCE spectrometer equipped with a multinuclear inverse probe. A spin-lock pulse of 400 ms was used. The number of scans per increment was 80, and 240 experiments were acquired in the second dimension. Total experimental time was approximately 8 h.

Modelling: All molecular mechanics calculations were carried out by using the AMBER* force field as implemented within Maestro/MacroModel 8.1. Standard potentials and atomic charges, as provided by the

AMBER* force field, were employed without modifications. AMBER* and OPLAA force fields produced essentially the same results in related structures. Calculations were initially performed under vacuum and then in chloroform (GB/SA solvation model). Most complex structures were virtually identical under both conditions. Energy minimizations were conducted over 500 iterations on a Silicon Graphics Origin 2000 Computer. Minimized structures were then subjected to conformational searches with 5000-step Monte Carlo multiple minimum simulations. All conformations within 15 kJ mol^{-1} of the computed global minimum were stored, and the representative lowest-energy structure was analysed.

Rate constants: The rate constants have been determined with the help of selective inversion-magnetisation transfer experiments (see the Supporting Information for an extended explanation). For the analysis of the results we have used the program CIFIT.[38] The relaxation delay was equal to five times the T_1 of the signals of interest. Typically, 17 or 22 data points were used for the fit, with the variable time delay increased from 1 ms to 4 s. Total experimental times were approximately 2–4 h. For the solutions of the samples in $CDCl_3$, the NH resonance at approximately 8.3 ppm (from **1a·1a·G**) was selectively inverted, and the evolution of this peak and the NH resonance at approximately 8.0 ppm (from **1a·1a**·$CDCl_3$) was followed. The number of scans per experiment was four or eight. In [D_8]toluene, the concentration of the empty capsule **1a·1a** was very low, or not detectable. Consequently, in this solvent the resonances from the free and encapsulated guest were used for the magnetisation transfer experiment. Inversion was carried out on the former. Due to the longer T_1 values of the involved peaks, only four scans per experiment were acquired.

The rate constants were determined at temperature intervals from 5 K. The range of temperatures investigated depended on the dynamic behaviour of the system (the rate constant had to be measurable, and the NMR signals resolved). These intervals were as follows: in $CDCl_3$: 238–273 K for **G** = CH_2Cl_2, 263–293 K for **G** = CH_3I and 243–273 K for **G** = CH_3NO_2; in [D_8]toluene: 238–273 K for **G** = CH_2Cl_2, 258–293 K for **G** = CH_3I and 233–268 K for **G** = CH_3NO_2.

Association constants: The association constants were determined from the integrals of the separate ^{1}H resonances for capsule and guest (see the Supporting Information). The number of scans was eight and the relaxation delay was equal to five times the T_1 of the guest. The average value from two different determinations was taken. The same temperatures as those used for determining the rate constants were investigated.

Acknowledgements

This work was supported by the Swiss National Science Foundation, the ETH Zurich, the Ministerio de Educación y Ciencia (MEC) of Spain (project CTQ2005-02323/BQU), and the Fundación Séneca-CARM (project PI-1/00749/FS/01). P.S.P. thanks the Swiss National Science Foundation, and the ETH Zurich for financial support. E.M.-V. thanks the Fundación Séneca-CARM for a grant. Both E.M.-V. and A.P. thank the MEC and the University of Murcia for their *Ramón y Cajal* contracts. R.-A.O. is grateful to the Fundación CajaMurcia for a fellowship.

[1] a) J. Rebek, Jr., *Chem. Soc. Rev.* **1996**, 255–264; b) M. M. Conn, J. Rebek, Jr., *Chem. Rev.* **1997**, *97*, 1647–1668; c) J. de Mendoza, *Chem. Eur. J.* **1998**, *4*, 1373–1377; d) J. Rebek, Jr., *Acc. Chem. Res.* **1999**, *32*, 278–286; e) C. A. Schalley, *Adv. Mater.* **1999**, *11*, 1535–1537; f) D. R. Turner, A. Pastor, M. Alajarín, J. W. Steed, *Struct. Bonding (Berlin)* **2004**, *108*, 97–168.

[2] a) F. Hof, S. L. Craig, C. Nuckolls, J. Rebek, Jr., *Angew. Chem.* **2002**, *114*, 1556–1578; *Angew. Chem. Int. Ed.* **2002**, *41*, 1488–1508; b) L. C. Palmer, J. Rebek, Jr., *Org. Biomol. Chem.* **2004**, *2*, 3051–3059.

[3] a) F. Hof, J. Rebek, Jr., *Proc. Nat. Acad. Sci. USA* **2002**, *99*, 4775–4777; b) A. Lützen, *Angew. Chem.* **2005**, *117*, 1022–1025; *Angew. Chem. Int. Ed.* **2005**, *44*, 1000–1002; c) J. Rebek, Jr., *Angew. Chem.* **2005**, *117*, 2104–2115; *Angew. Chem. Int. Ed.* **2005**, *44*, 2068–2078.

[4] a) N. Branda, R. Wyler, J. Rebek, Jr., *Science* **1994**, *263*, 1267–1268; b) J. Kang, J. Rebek, Jr., *Nature* **1996**, *382*, 239–241; c) O. Mogck, M. Pons, V. Böhmer, W. Vogt, *J. Am. Chem. Soc.* **1997**, *119*, 5706–5712; d) R. Meissner, X. Garcias, S. Mecozzi, J. Rebek, Jr., *J. Am. Chem. Soc.* **1997**, *119*, 77–85; e) T. Szabo, G. Hilmersson, J. Rebek, Jr., *J. Am. Chem. Soc.* **1998**, *120*, 6193–6194; f) M. O. Vysotsky, I. Thondorf, V. Böhmer, *Angew. Chem.* **2000**, *112*, 1309–1312; *Angew. Chem. Int. Ed.* **2000**, *39*, 1264–1267; g) F. Hof, C. Nuckolls, S. L. Craig, T. Martín, J. Rebek, Jr., *J. Am. Chem. Soc.* **2000**, *122*, 10991–10996.

[5] a) M. Alajarín, A. López-Lázaro, A. Pastor, P. D. Prince, J. W. Steed, R. Arakawa, *Chem. Commun.* **2001**, 169–170; b) M. Alajarín, A. Pastor, R.-A. Orenes, J. W. Steed, *J. Org. Chem.* **2002**, *67*, 7091–7095; c) M. Alajarín, A. Pastor, R.-A. Orenes, J. W. Steed, R. Arakawa, *Chem. Eur. J.* **2004**, *10*, 1383–1397; d) M. Alajarín, A. Pastor, R.-A. Orenes, E. Martínez-Viviente, P. S. Pregosin, *Chem. Eur. J.* **2006**, *12*, 877–886.

[6] a) D. S. Lawrence, T. Jiang, M. Levett, *Chem. Rev.* **1995**, *95*, 2229–2260; b) L. J. Prins, D. N. Reinhoudt, P. Timmerman, *Angew. Chem.* **2001**, *113*, 2446–2492; *Angew. Chem. Int. Ed.* **2001**, *40*, 2382–2426.

[7] a) E. O. Stejskal, J. E. Tanner, *J. Chem. Phys.* **1965**, *42*, 288–292; b) P. Stilbs, *Prog. Nucl. Magn. Reson. Spectrosc.* **1987**, *19*, 1–45; c) W. S. Price, *Annu. Rep. NMR Spectrosc.* **1996**, *32*, 51–142; d) C. S. Johnson, Jr., *Prog. Nucl. Magn. Reson. Spectrosc.* **1999**, *34*, 203–256.

[8] a) L. Frish, S. E. Matthews, V. Böhmer, Y. Cohen, *J. Chem. Soc. Perkin Trans. 2* **1999**, 669–671; b) L. Frish, M. O. Vysotsky, S. E. Matthews, V. Böhmer, Y. Cohen, *J. Chem. Soc. Perkin Trans. 2* **2002**, 88–93; c) L. Avram, Y. Cohen, *Org. Lett.* **2002**, *4*, 4365–4368; d) L. Avram, Y. Cohen, *J. Am. Chem. Soc.* **2002**, *124*, 15148–15149; e) L. Avram, Y. Cohen, *Org. Lett.* **2003**, *5*, 1099–1102; f) L. Frish, M. O. Vysotsky, V. Böhmer, Y. Cohen, *Org. Biomol. Chem.* **2003**, *1*, 2011–2014; g) Y. Cohen, L. Avram, L. Frish, *Angew. Chem.* **2005**, *117*, 524–560; *Angew. Chem. Int. Ed.* **2005**, *44*, 520–554.

[9] a) S. Forsén, R. A. Hoffman, *J. Chem. Phys.* **1963**, *39*, 2892–2901; b) R. A. Hoffman, S. Forsén, *Prog. Nucl. Magn. Reson. Spectrosc.* **1966**, *1*, 15–204; c) J. J. Led, H. Gesmar, *J. Magn. Reson.* **1982**, *49*, 444–463; d) A. D. Bain, D. A. Fletcher, *Mol. Phys.* **1998**, *95*, 1091–1098.

[10] The resonances for **1a·1a**·$CDCl_3$ in this mixture were assigned by comparison with the spectrum of **1a·1a** at 213 K in $CDCl_3$ (in the absence of guest).

[11] The assignment of the N^1–H protons (see Scheme 1) to the resonance at higher frequency, approximately 8 ppm, was based on the X-ray structure of **1a·1a** ($d(N^1\cdots O{=}C) < d(N^2\cdots O{=}C)$) and further confirmed on the basis of a ^{1}H,^{1}H ROESY spectrum measured for a sample in the presence of CH_2Cl_2 at 213 K (see below).

[12] a) The guest was added in a 30-fold excess; b) volume calculated with Hyperchem 6.01.

[13] The ^{1}H NMR measurements were conducted at 300 ($C_2D_2Cl_4$ and [D_8]toluene), 243 ($C_2D_2Cl_4$) and 213 K ([D_8]toluene).

[14] a) It is difficult to determine whether these dimers are truly empty or filled by molecules from atmospheric gases; b) we have not been able to observe a signal corresponding to H_2O encapsulated inside **1a·1a**.

[15] These experiments were conducted by addition of a 20- to 100-fold excess of guest **G** (0.09–0.67 M) to a solution of **1a·1a** in [D_8]toluene (3–6 mM).

[16] For all the guests investigated, the maximum difference in $\delta(^1H)$ between the encapsulated guest in $CDCl_3$ and [D_8]toluene is 0.35 ppm (at 213 K). When **G** = $CHCl_3$ and C_6H_6 these resonances of **G** are overlapped with resonances from **1a·1a** and **1a·1a·G**, and thus, are not observable.

[17] Aromatic solvent-induced shift (ASIS). For instance, see: M. Ahmad, L. Phillips, *J. Chem. Soc. Perkin Trans. 2* **1977**, 1656–1661.

[18] These NOE contacts are not present in the ROESY spectrum of **1a** in [D_6]DMSO in which the compound exists as a non-assembled monomer (Supporting Information).

[19] The Stokes–Einstein equation is $D=(k_BT)/(6\pi\eta r_H)$, in which D is the diffusion coefficient, k_B is the Boltzmann constant, T is the temperature in Kelvin, η is the viscosity of the solution at the temperature T (for diluted solutions, the viscosity of the solvent can be used), and r_H is the hydrodynamic radius (the radius of a hypothetical hard sphere that diffuses with the same speed as the particle under examination). For instance, see: J. T. Edward, *J. Chem. Educ.* **1970**, *47*, 261–270. The viscosities have been taken from C. L. Yaws, *Chemical Properties Handbook*, McGraw-Hill, New York, **1999**, with the exception of the viscosity for toluene at 213 K, which is erroneous in that reference and has been taken from W. Fieggen, H. Gerding, *Recl. Trav. Chim. Pays-Bas* **1970**, *89*, 236–244. It is accepted that the factor 6 in the Stokes–Einstein equation is not valid for small species that are comparable in size to the solvent molecules. The limits for this condition are not clear, but in general when $r_{solute}/r_{solvent} \leq \approx 2$, the substitution of 6 by 4, or its multiplication by an empirical factor $f<1$ has been proposed. For instance, see: A. Gierer, K. Wirtz, *Z. Naturforsch. A.* **1953**, *8*, 532–538; A. Spernol, K. Wirtz, *Z. Naturforsch. A.* **1953**, *8*, 522–532; H. C. Chen, S. H. Chen, *J. Phys. Chem.* **1984**, *88*, 5118–5121; J. T. Edward, *J. Chem. Educ.* **1970**, *47*, 261–270; M. Ue, *J. Electrochem. Soc.*, **1994**, *141*, 3336–3342. To be consistent and facilitate comparison, we have used the Stokes–Einstein equation with the factor 6. However, for the small solvent and guest molecules, we show in parentheses in Tables 3 and 4 the radii calculated by using the empirical equation proposed by Chen et al. $f=1/[1+\{0.695(r_{solv}/r_{solute})^{2.234}\}]$.

[20] For elongated molecules the hydrodynamic radius can be considered to be approximately 85% of the rotational radius, according to a suggestion from Mattison et al. in: K. W. Mattison, U. Nobbmann, D. Dolak, *Am. Biotechnol. Lab.* **2001**, *19*, 66–67. For **1a·1a**, the rotational radius estimated by measuring distances between atoms in the X-ray structure is approximately 10.5 Å. 85% of this value would be 9.0 Å.

[21] a) The small difference between the r_H values at 300 and 213 K can be due to errors in the viscosities used in the Stokes–Einstein equation; b) no empirical equations have been suggested to modify the Stokes–Einstein equation for small molecules at low temperatures; c) the absence of convection effects at low temperature has been checked by repeating the diffusion measurements with different diffusion times, as explained in ref. [37]. The perfect agreement and reproducibility between the different samples provides an additional check on the quality of our low temperature measurements.

[22] η(DMSO) at 300 K $= 1.9075\times10^{-3}$ Kg s^{-1} m^{-1}.

[23] The calculated structure for **1b·1b·**CH_2Cl_2 is in good agreement with its solid-state structure determined by X-ray diffraction (see ref. [5b]).

[24] a) J. Canceill, L. Lacombe, A. Collet, *J. Am. Chem. Soc.* **1986**, *108*, 4230–4232; b) J. Canceill, M. Cesario, A. Collet, J. Guilhem, L. Lacombe, B. Lozach, C. Pascard, *Angew. Chem.* **1989**, *101*, 1249–1251; *Angew. Chem. Int. Ed. Engl.* **1989**, *28*, 1246–1248.

[25] S. Mecozzi, J. Rebek, Jr., *Chem. Eur. J.* **1998**, *4*, 1016–1022.

[26] B. C. Hamann, K. D. Shimizu, J. Rebek, Jr., *Angew. Chem.* **1996**, *108*, 1425–1427; *Angew. Chem. Int. Ed. Engl.* **1996**, *35*, 1326–1329.

[27] T_c is the compensation temperature, see: a) R. Lumry, S. Rajender, *Biopolymers* **1970**, *9*, 1125–1227; b) K. N. Houk, A. G. Leach, S. P. Kim, X. Zhang, *Angew. Chem.* **2003**, *115*, 5020–5046; *Angew. Chem. Int. Ed.* **2003**, *42*, 4872–4897.

[28] a) J. D. Dunitz, *Chem. Biol.* **1995**, *2*, 709–712; b) M. S. Searle, M. S. Westwell, D. H. Williams, *J. Chem. Soc. Perkin Trans. 2* **1995**, 141–151; c) E. Grunwald, C. Steel, *J. Am. Chem. Soc.* **1995**, *117*, 5687–5692.

[29] It cannot be disregarded that the correlation could be due to the interrelated errors in ΔH and ΔS, as pointed out in ref. [27b].

[30] a) R. G. Chapman, J. C. Sherman, *J. Am. Chem. Soc.* **1998**, *120*, 9818–9826; b) M. V. Rekharsky, Y. Inoue, *Chem. Rev.* **1998**, *98*, 1875–1917; c) E. L. Piatnitski, R. A. Flowers II, K. Deshayes, *Chem. Eur. J.* **2000**, *6*, 999–1006.

[31] When the capsules **1a·1a** and **1c·1c** are mixed in solution, the heterodimer **1a·1c** is formed. The three species coexist in a 1:1:2 ratio. See ref. [5b].

[32] a) T. Szabo, B. M. O'Leary, J. Rebek, Jr., *Angew. Chem.* **1998**, *110*, 3606–3609; *Angew. Chem. Int. Ed.* **1998**, *37*, 3410–3413; b) X. Wang, K. N. Houk, *Org. Lett.* **1999**, *1*, 591–594.

[33] J. Santamaría, T. Martín, G. Hilmersson, S. L. Craig, J. Rebek, Jr., *Proc. Natl. Acad. Sci. USA* **1999**, *96*, 8344–8347.

[34] S. L. Craig, S. Lin, J. Chen, J. Rebek, Jr., *J. Am. Chem. Soc.* **2002**, *124*, 8780–8781.

[35] a) P. S. Pregosin, E. Martínez-Viviente, P. G. A. Kumar, *Dalton Trans.* **2003**, 4007–4014; b) P. S. Pregosin, P. G. A. Kumar, I. Fernández, *Chem. Rev.* **2005**, *105*, 2977–2998.

[36] H. J. V. Tyrrell, K. R. Harris, *Diffusion in Liquids*, Butterworths, London, **1984**.

[37] E. Martínez-Viviente, P. S. Pregosin, *Helv. Chim. Acta* **2003**, *86*, 2364–2378.

[38] Developed by Alex D. Bain, McMaster University, Hamilton, Ontario, Canada, www.chemistry.mcmaster.ca/bain/.

Received: August 30, 2006
Published online: November 9, 2006

